HIFI ICC note

Subject: Empirical Examination of Possible H/V Imbalance
By: Schuyler Van Dyk, Pat Morris, Scott Jones
Date: 1 February 2016

1 Examination of H/V Imbalance for a Large Sample

Imbalance in the spectral line strengths measured through the H and V polarization mixer beams has been known to occur since PV. Random pointing errors can cause this imbalance. A systematic offset in the SIAM, which is suspected for some bands, can also be a cause. For a large enough set of observations of compact-like line sources, we should expect to detect H/V imbalances from offsets of ~2" or more, or otherwise verify that it is not important.

Executive summary: The empirical results we find for the mean of the ratio ρ_{HV} are entirely consistent with the quantitative impact of the calculated SIAM biases on H/V imbalances for compact sources.

2 Extraction of the Sample

We considered the total set of 7518 Point mode obsids in all bands. We constructed a script for HIPE that ran on all WBS data at Level 2.5 from our HIFI database at the NHSC. In the script we applied the GaussLike class to both the H and V polarizations for both the upper and lower sidebands. (GaussLike is invoked initially in the SpectrumFitter GUI in HIPE.) GaussLike does a quick *automatic* fit to the strongest "Gaussian-Like" feature, either in emission or absorption, in each spectrum, and returns the estimation of the peak amplitude, the line center, and the line width. The script then computes the ratio of the peak for H and for V in each sideband for each spectrum. If GaussLike cannot readily find a peak for a spectrum, it assigns the value of the peak to be exactly 1.0.

We considered a "good" value of the H/V ratio for a given sideband to be when the H and V line centers agreed to $\Delta v \leq 5$ MHz; in this case, we assigned a flag of '0' to the sideband. Sidebands for which the line center difference $\Delta v > 5$ MHz were assigned a flag '9999'. Sidebands for which the peak was assigned value 1.0 were flagged as '1111'.

The demographics of the 7518 total obsids were 36.0% with flags '0','0'; 6.6% with flags '1111','1111'; 1.7% with flags '9999','0'; 1.6% with flags '0','9999'; and, 53.6% with flags '9999','9999'. An example of the last case is shown in `Figure 1`. That is, somewhat more than half of the obsids were not useful for our analysis. We show in `Figure 2` a histogram of the quantity deltaU = | centerHU – centerVU |, where centerHU and centerVU are the line centers for the two polarizations for the upper sideband. The takeaway is that we obtained a significant number of obsids with flag ‘0’,’0’.

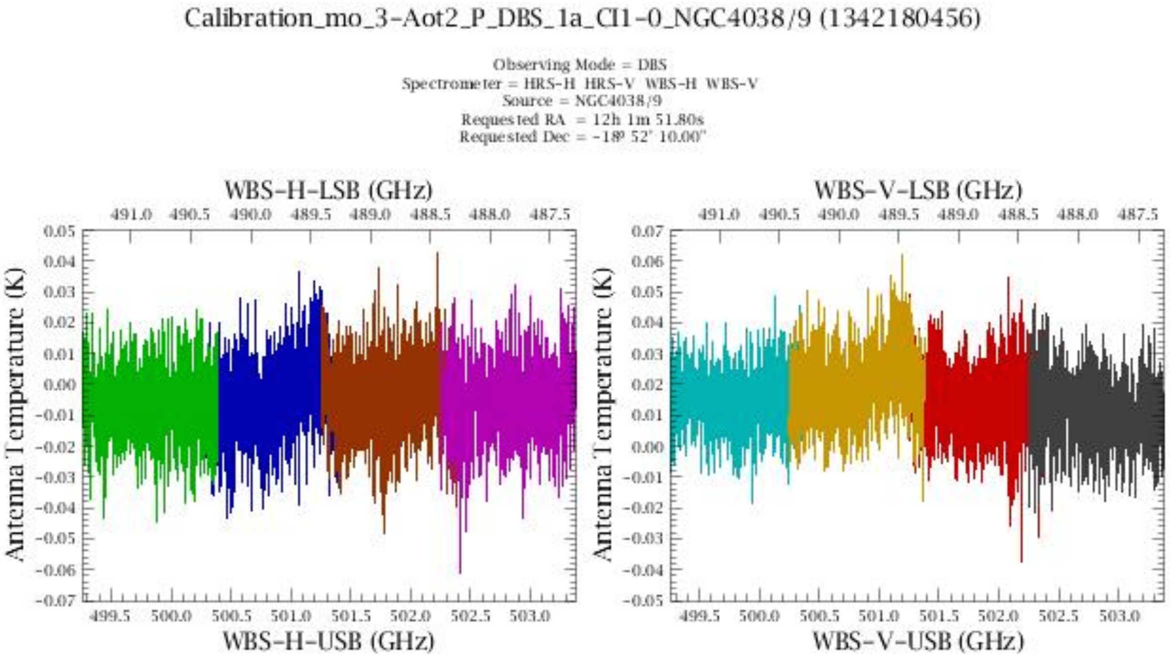

Figure 1: An example of an obsid flagged as '9999', '9999', for which GaussLike tried to fit random noise spikes. Some, but certainly not all, of the spectra flagged in this way are of a relatively low signal-to-noise ratio (S/N), such as the one shown.

A benefit of having used GaussLike is that it, generally, reliably finds a line’s true peak flux and does so automatically. One drawback of GaussLike is that the continuum level for the line peak fit is always assumed by the algorithm to be zero. Another drawback is that GaussLike does not always reliably find the line’s center. Additionally, the ‘1111’ flag arises because GaussLike is not a perfect algorithm, since sometimes it fails to fit what looks to an otherwise “normal” emission feature. See Figure 3.

GaussLike will also assign a value to the width of exactly 1.0 if it cannot readily determine the line width for a spectrum, and we therefore eliminated those obsids. We then hand-inspected the remaining obsids in each band. We weeded out those obsids for which the combined flags for both sidebands were ‘0,0’, but for which the line fits were to absorption features or to obvious noise peaks. We weeded out obsids with flagged spur candidates. We weeded out obsids with spectra having flagged bad or saturated pixels. We also threw out obsids for which the ratio of the fitted lines widths in the two polarizations diverged significantly from unity, since it was visually not clear if the line in each polarization was actually being fitted correctly and may just be adding noise to the statistics.

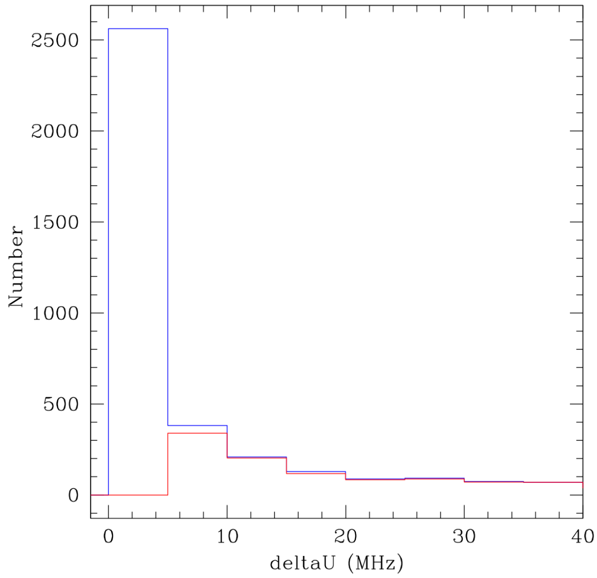

Figure 2: Histogram of the quantity deltaU = | centerHU – centerVU | (where centerHU and centerVU are the line centers, as measured by GaussLike, for the two polarizations for the upper sideband) for obsids with flag '0','0' (blue line) and with flag '9999','9999' (red line). Obsids with flag '1111','1111' have been excluded. The shape of the tail of the '0','0' distribution is similar to that of the '9999','9999' distribution for 5 MHz < deltaU < ~10 MHz.

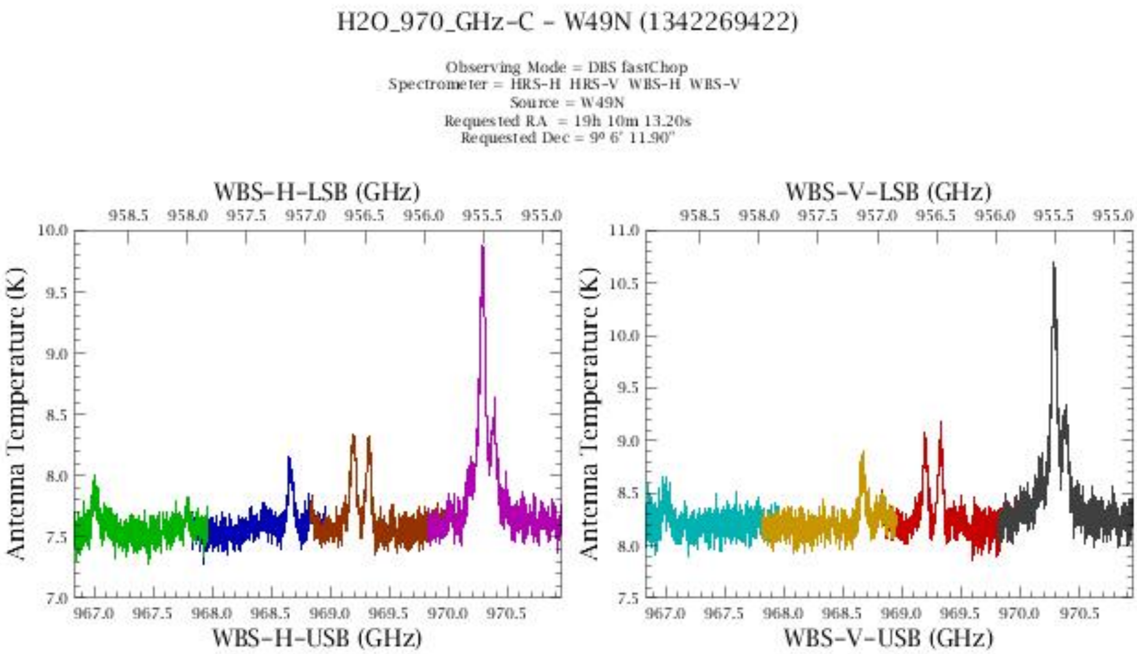

Figure 3: An example of an obsid flagged as '1111', '1111', for which GaussLike, for whatever reason, could not fit a peak to an otherwise, high S/N emission feature. Measuring this ratio by hand using the SpectrumFitterGUI shows that GaussLike, in this case, first needed a non-zero continuum (polynomial) fit, before it could automatically fit the highest peak. The by-hand ratio for the LSB is 0.892, slightly less than, but roughly consistent with the statistics for Band 4.

3 Results

3.1 Correlation of H/V imbalance with OD

We find, not surprisingly, that the H/V ratio is essentially the same for each sideband, and we adopt the upper sideband and define this as ρ_{HV}. We initially looked for any correlation of ρ_{HV} with observation date OD for all bands. We show this relationship in **Figure 4**. The dot-dashed lines correspond to the epochs of SIAM adjustments. The dotted lines correspond to OD-762, application of the focal length correction; OD-866, the 1-D distortion correction; OD-1011, the n-D distortion correction; and, OD-1034, the guide star catalog clean-up. We do not find a readily evident correlation of ρ_{HV} with OD. All of these points use the same version of the SIAM, so the lack of any observable differences with OD can be taken as an expected result, and that nothing weird with the telescope (e.g., STR biases) is detected.

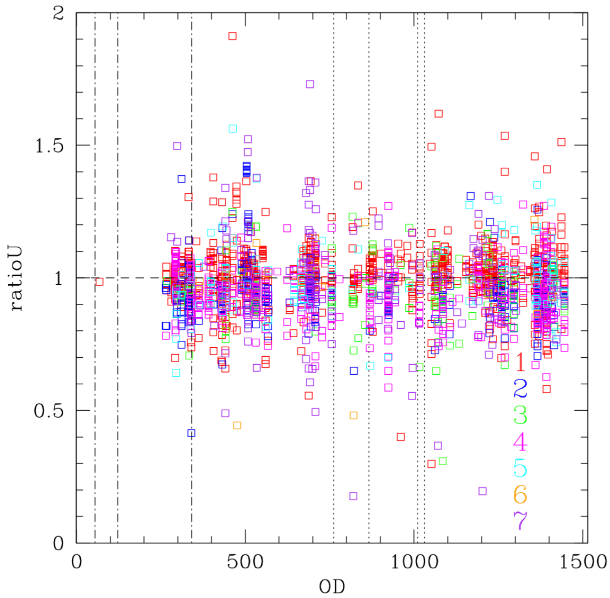

Figure 4: Distribution of the ratio of the line peak in H to V for the upper sideband, ratioU = $(H/V)_{upper}$, with observation date OD. Bands 1-7 have been indicated by different colored open squares.

3.2 Correlation of H/V imbalance with Pointing Offset

Next, we examined any correlation of ρ_{HV} with the offset, Δ, between the expected and reconstructed pointing, (raNominal, decNominal) and (ra, dec), respectively. The offset is defined as Δ = sqrt(((cos[dec]*(ra-raNominal))^2 + (dec-decNominal)^2). We show this distribution in **Figure 5** for Bands 1 and 7. The relationship in the other bands looks similar. Again, we see no obvious correlation with Δ.

3.3 Correlation of H/V imbalance with Position Angle

Finally, we explored any relationship of ρ_{HV} with observing position angle, posAngle. We show these distributions in all bands in **Figure 6** through **Figure 12.** We have broken out the distributions by subband in these figures. In essence, although there may be a *weak* correlation of ρ_{HV} with posAngle --- see **Table 1** --- these ensemble distributions serve to demonstrate the overall offset of the ratio ρ_{HV} with respect to unity for each band.

We summarize the overall statistics of ρ_{HV} for each band in **Table 2.** Band 6 does not have enough statistics to allow a meaningful conclusion to be drawn.

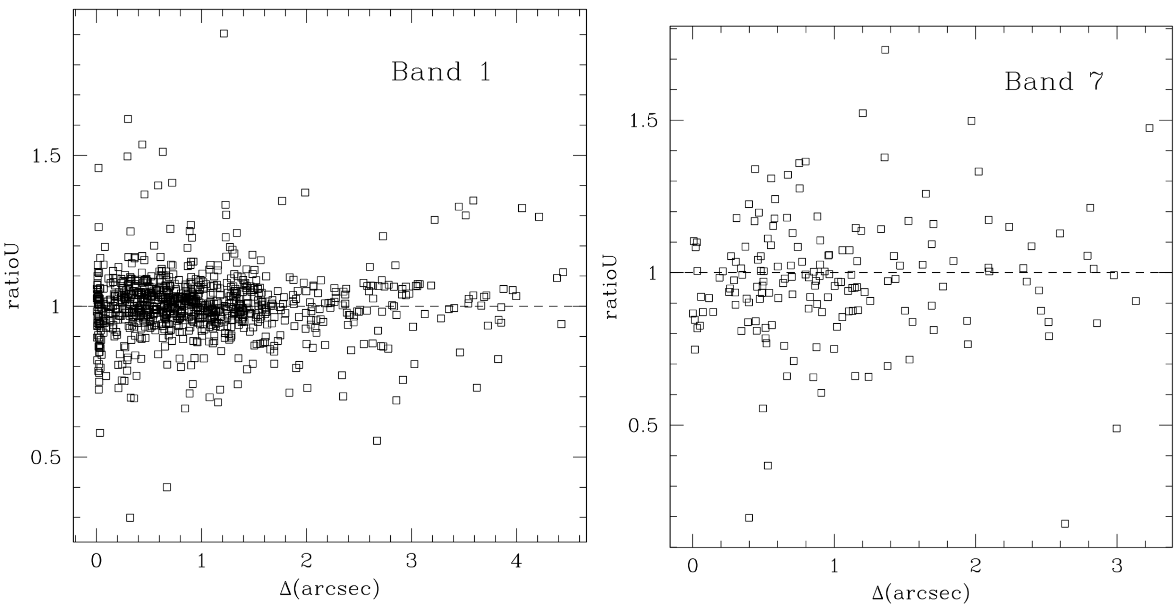

Figure 5: Distribution of the ratio of the line peak in H to V for the upper sideband, ratioU = $(H/V)_{upper}$, with pointing offset, Δ, for Bands 1 (left) and 7 (right).

Table 1: Statistics of ρ_{HV} for each band for each of the groupings by posAngle

	posAngle < 180				***posAngle > 180***			
Band	**No. of obsids**	**Mean**	**StDev**	**Median**	**No. of obsids**	**Mean**	**StDev**	**Median**
1	538	1.007	0.112	1.007	414	1.006	0.114	1.010
2	196	0.950	0.139	0.922	132	0.930	0.082	0.926
3	74	0.963	0.113	0.957	72	0.945	0.112	0.945
4	241	0.956	0.101	0.947	159	0.916	0.102	0.923
5	60	1.013	0.126	0.993	54	0.978	0.149	0.956
6	…	…	…	…	…	…	…	…
7	97	0.980	0.219	0.994	78	0.974	0.194	0.957

Table 2: Overall statistics of ρ_{HV} for each band

Band	No. of obsids	Mean	StDev	Median
1	952	1.007	0.113	1.008
2	328	0.942	0.119	0.923
3	146	0.954	0.112	0.950
4	400	0.941	0.103	0.939
5	114	0.996	0.138	0.984
6	20	0.960	0.195	0.987
7	175	0.977	0.208	0.980

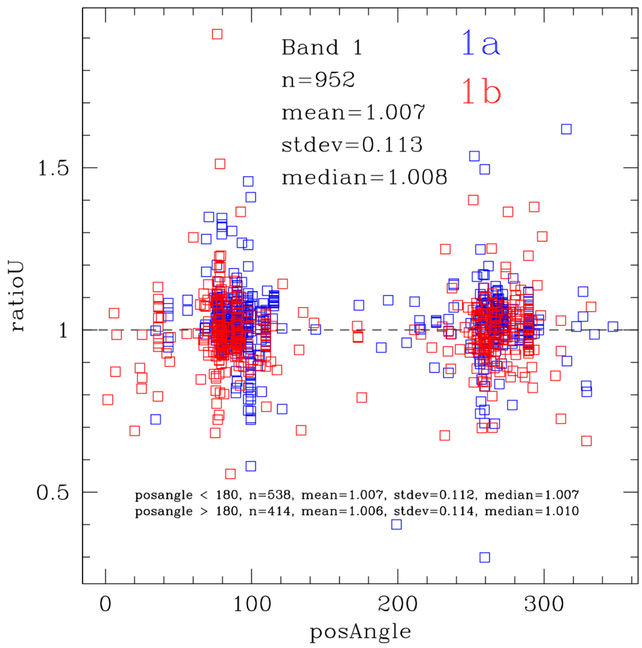

Figure 6: Distribution of the ratio of the line peak in H to V for the upper sideband, ratioU = $(H/V)_{upper}$, with position angle posAngle for Band 1. Subbands a and b are blue and red symbols, respectively.

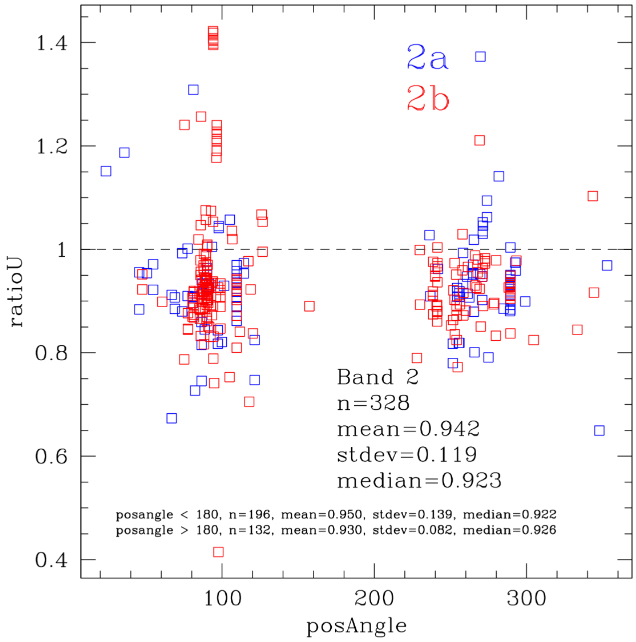

Figure 7: Distribution of the ratio of the line peak in H to V for the upper sideband, ratioU = $(H/V)_{upper}$, with position angle posAngle for Band 2. Subbands a and b are blue and red symbols, respectively.

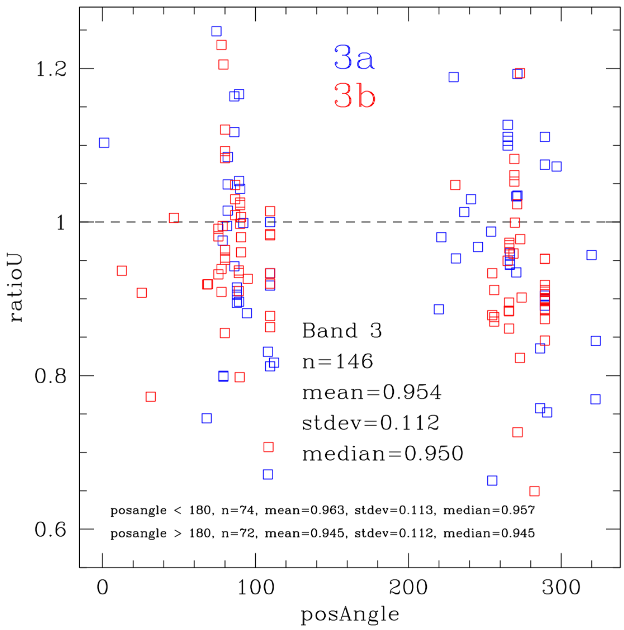

Figure 8: Distribution of the ratio of the line peak in H to V for the upper sideband, ratioU = $(H/V)_{upper}$, with position angle posAngle for Band 3. Subbands a and b are blue and red symbols, respectively.

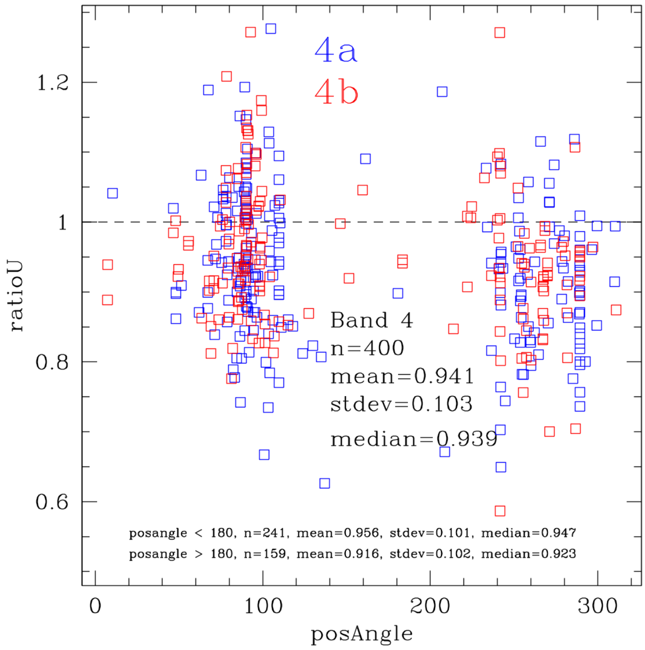

Figure 9: Distribution of the ratio of the line peak in H to V for the upper sideband, ratioU = $(H/V)_{upper}$, with position angle posAngle for Band 4. Subbands a and b are blue and red symbols, respectively.

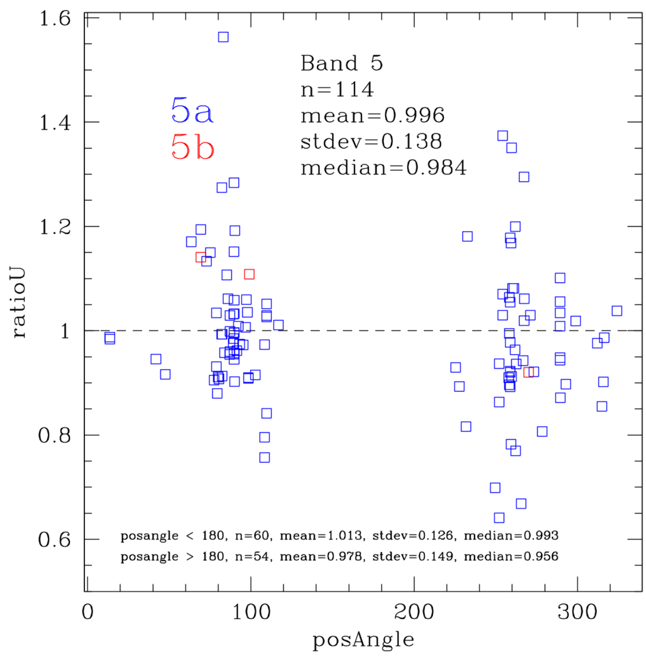

Figure 10: Distribution of the ratio of the line peak in H to V for the upper sideband, ratioU = $(H/V)_{upper}$, with position angle posAngle for Band 5. Subbands a and b are blue and red symbols, respectively.

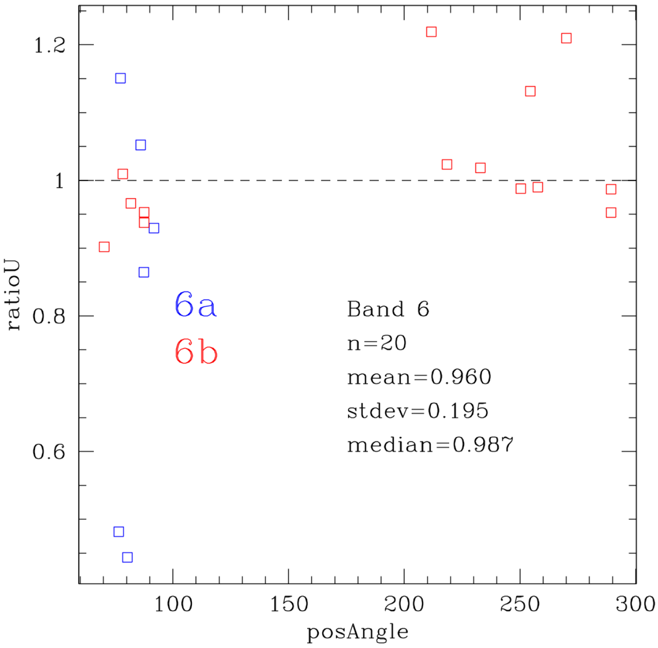

Figure 11: Distribution of the ratio of the line peak in H to V for the upper sideband, ratioU = $(H/V)_{upper}$, with position angle posAngle for Band 6. Subbands a and b are blue and red symbols, respectively.

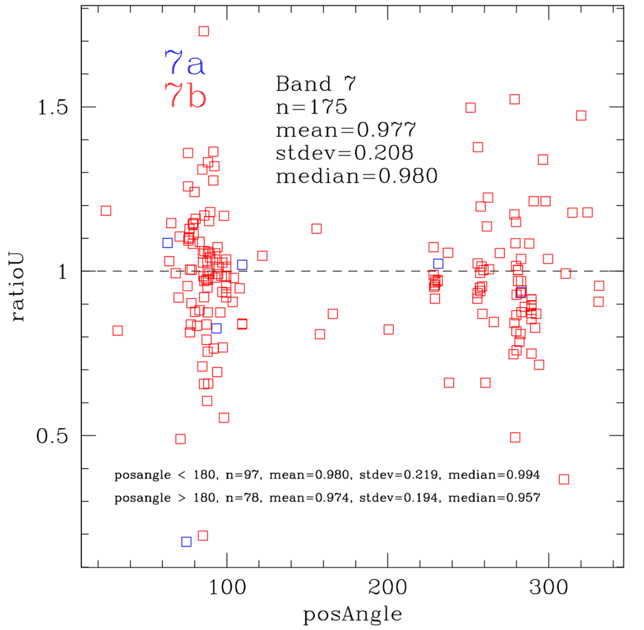

Figure 12: Distribution of the ratio of the line peak in H to V for the upper sideband, ratioU = $(H/V)_{upper}$, with position angle posAngle for Band 7. Subbands a and b are blue and red symbols, respectively.

4 Conclusions

The median value of ρ_{HV} for Band 1 is essentially unity. Noticeable offsets from unity can be seen for Bands 2, 3, and 4, and less obviously, for Bands 5 and 7. The mean and median values for ρ_{HV} appear to all be <1, implying that line peaks in the V polarization tend to be higher than in H. Possible differences in ρ_{HV} may be seen for obsids observed at posAngle ≈90° and posAngle ≈270° for Bands 3, 4, 5, and, possibly, 7. Generally, there are not enough statistics for Band 6 to be highly conclusive.

The dispersions in ρ_{HV} are certainly large enough that the mean values agree with those calculated for a compact source by W. Jellema which are reproduced below from the HIFI Handbook (draft version):

Band	θ_b (arcsec)	$\Delta\theta_0^H$ (arcsec)	$\Delta\theta_0^V$ (arcsec)	$\langle\eta_H\rangle$	$\langle\eta_V\rangle$	$\langle\rho_{HV}\rangle$	σ_ρ
1	33.0	4.1	3.4	0.95	0.97	0.98	0.03
2	26.6	4.1	1.4	0.93	0.98	0.94	0.03
3	22.1	4.4	2.1	0.89	0.96	0.92	0.07
4	18.9	3.6	0.4	0.89	0.98	0.91	0.05
5	17.3	0.8	3.3	0.97	0.89	1.10	0.06
6	12.4	2.0	2.6	0.90	0.85	1.05	0.03
7	11.2	3.2	2.3	0.76	0.85	0.90	0.04

Impact of SIAM bias errors on the scientific calibration of H and V line intensities.

The median values of ρ_{HV} that we have measured generally agree with the mean values calculated by Jellema, except for Bands 5a, 6, and 7; there are no statistics for Band 5b, and again, the statistics are too small in Band 6 to be conclusive, and we note that the median for Band 7 only slightly disagrees with the calculated mean. We have hand-inspected ~35 obsids in Band 5a, checking the results for ρ_{HV}. The general trend for this band is verified, so we continue to find from this inspection that ρ_{HV} for Band 5 disagrees with the predicted value. We note that occasionally there will be large differences between continuum levels for a given obsid that might drive up (or down) the value of ρ_{HV}, but this is generally true for all of the bands. Within Band 5a, which also has relatively low number statistics, it is conceivable that there is a bias from the kind of sources that were observed, i.e., non-compact (which should drive the ratio towards unity), or a weighting towards specific sources with an emitting source offset from even an ideal pointing to the synthetic aperture. This aspect has not been thoroughly investigated, but see results of follow-up on IRC+10216, below. Thus, with the exception of Band 5, though, all of the measured values of ρ_{HV} are consistent with expectation of a SIAM bias.

The vertical spread around the mean in each band has several possible explanations, qualitatively summarized here. First, there are possible erroneous values of ρ_{HV} obtained in the lights-out fits via GaussLike (although, we did a fair amount of spot-check confirmation by hand). These are among the several-σ outliers. Second, if we interpret the mean values to reflect average emitting source properties, thus implying a compact size more often than extended in each band, then departures from the mean must occur for extended sources. This should drive or skew ρ_{HV} to unity, thus the distribution around the mean is not expected to be

Gaussian (underneath the GaussLike fit errors). Finally, even with an error-free SIAM, there was no guarantee that the observer knew or entered the correct coordinates of the emitting source that should be pointed at with the synthetic apertures, thus we can anticipate the effects of a range of unaccounted-for differential aspect angles and distances to both beam centers when the emitting source does not fill the beam.

4.1 H/V imbalance Statistics for IRC +10216

Interestingly, if we isolate just the numerous obsids of the carbon star IRC +10216 (CW Leo) made in each of the bands (although only 2 obsids are available for Band 6), we can see a far better agreement in (particularly the median value of) ρ_{HV} with the calculated values, especially for Band 5. See **Table 3**. These values more evidently imply that the ratio may well be driven by biases in the SIAM in each band.

Table 3: Statistics of ρ_{HV} for the source IRC +10216 in the upper sideband of each band

Band	**No. of obsids**	**Mean**	**StDev**	**Median**
1	76	1.007	0.053	1.001
2	43	0.918	0.034	0.924
3	31	0.958	0.139	0.911
4	35	0.911	0.087	0.902
5	12	1.046	0.145	1.032
6	2	0.970	0.024	0.970
7	10	0.880	0.069	0.884